PLOS ONE

RESEARCH ARTICLE

Magnetic Resonance Imaging Is Sensitive to Pathological Amelioration in a Model for Laminin-Deficient Congenital Muscular Dystrophy (MDC1A)

Ravneet Vohra[2‡], Anthony Accorsi[1‡], Ajay Kumar[1‡], Glenn Walter[2], Mahasweta Girgenrath[1]*

1 Department of Health Sciences, Sargent College, Boston University, Boston, MA, United States of America, **2** Department of Physiology and Functional Genomics, College of Medicine, University of Florida, Gainesville, FL, United States of America

‡ These authors are equal authors on this work.
* swetag@bu.edu

Citation: Vohra R, Accorsi A, Kumar A, Walter G, Girgenrath M (2015) Magnetic Resonance Imaging Is Sensitive to Pathological Amelioration in a Model for Laminin-Deficient Congenital Muscular Dystrophy (MDC1A). PLoS ONE 10(9): e0138254. doi:10.1371/journal.pone.0138254

Editor: Ashok Kumar, University of Louisville School of Medicine, UNITED STATES

Received: May 20, 2015

Accepted: August 27, 2015

Published: September 17, 2015

Data Availability Statement: All relevant data are within the paper.

Funding: This work was supported with the research grants awarded to M.G. from Cure CMD, Struggle Against Muscular Dystrophy (SAM), Muscular Dystrophy Association (218938), the Paul D. Wellstone Muscular Dystrophy Cooperative Research Center (U54AR052646) and the National High Magnetic Field Laboratory, which is supported by NSF DMR-1157490 and the State of Florida.

Abstract

Purpose

To elucidate the reliability of MRI as a non-invasive tool for assessing in vivo muscle health and pathological amelioration in response to Losartan (Angiotensin II Type 1 receptor blocker) in DyW mice (mouse model for Laminin-deficient Congenital Muscular Dystrophy Type 1A).

Methods

Multiparametric MR quantifications along with histological/biochemical analyses were utilized to measure muscle volume and composition in untreated and Losartan-treated 7-week old DyW mice.

Results

MRI shows that DyW mice have significantly less hind limb muscle volume and areas of hyperintensity that are absent in WT muscle. DyW mice also have significantly elevated muscle levels (suggestive of inflammation and edema). Muscle T_2 returned to WT levels in response to Losartan treatment. When considering only muscle pixels without T_2 elevation, DyW T_2 levels are significantly lower than WT (suggestive of fibrosis) whereas Losartan-treated animals do not demonstrate this decrease in muscle T_2. MRI measurements suggestive of elevated inflammation and fibrosis corroborate with increased Mac-1 positive cells as well as increased Picrosirius red staining/COL1a gene expression that is returned to WT levels in response to Losartan.

Competing Interests: The authors have declared that no competing interests exist.

Conclusions

MRI is sensitive to and tightly corresponds with pathological changes in DyW mice and thus is a viable and effective non-invasive tool for assessing pathological changes.

Introduction

Congenital muscular dystrophy (CMD) is a heterogeneous group of neuromuscular disorders that result from defects in proteins related to the dystrophin-glycoprotein complex (DGC). The DGC is an integral part of the muscle membrane and is responsible for membrane stability as well as signal transduction [1]. Laminin-deficient CMD type 1A (MDC1A) is an autosomal recessive disease caused by mutations in the LAMA2 gene that encodes for the alpha two chain of the muscle- and Scwhann cell-specific heterotrimeric extracellular matrix protein Laminin-211 [2]. Absence of a functional copy of this protein results in defective myofiber anchoring and vast signaling dysregulation that manifests in a multitude of secondary pathologies, including failed regeneration, inflammation, fibrosis, apoptosis, and necrosis [3, 4]. Children with this disease present at/soon after birth with severe weakness, atrophy and hypotonia, and ultimately die prematurely due to respiratory complications or failure to thrive [5].

The current gold standard for visualization of muscle pathology is biopsy. While informative, it provides only a limited sampling of the entire muscle and is considered invasive and potentially painful. Furthermore, effective preclinical studies often rely on histological analyses of a muscle post-euthanasia, hence establishing a non-invasive method to track therapeutic progress would be incredibly beneficial to preclinical research in addition to patient care.

Over the last two decades, magnetic resonance imaging (MRI) has emerged as an important tool in muscle research. This has been particularly true in the realm of muscular dystrophy, where it has been shown in Duchenne muscular dystrophy (DMD) that MRI is a valuable tool for in vivo monitoring of muscle health and disease progression [6, 7]. By exploiting the intrinsic MR relaxation properties, muscle size and composition can be reliably determined. For example, 3D T_1-weighted (T_1w) images can be used to generate high-resolution measurements of muscle volumes and cross-sectional areas while T_2-weighted (T_2w) MRIs can be used to further delineate between muscle, fat, and inflammation/edema [7].

The Lama2$^{Dyw-/+}$ (DyW) mouse model is the most commonly studied animal model for MDC1A. Unlike the *mdx* mouse model frequently utilized in DMD research, DyW mice exhibit a more severe phenotype and rarely survive past 2 months [8–10]. Because of their stunted growth and frailty, these mice can present inherent challenges for MR imaging. While initial observations were made on the larger and less severe Dy/Dy model of MDC1A by Tardif de Gery *et. al* in 2000, the present study shows for the first time that it is not only possible to detect the underlying DyW pathology, but also that MRI can be used to detect therapeutic improvements in DyW muscles (in this case in response to the Angiotensin II type 1 receptor blocker, Losartan). Most importantly, MR indices coincide with biochemical and histological analyses and thus further validate the use of MRI as a viable and effective biomeasure for preclinical studies, even in very aggressive scenarios.

Materials and Methods

Animals

Heterozygous B6.129 Lama2$^{dy\text{-}W/+}$ (DyW) mice carrying a mutation in the LAMA2 gene were kindly provided by Dr. Eva Engvall (Burnham Institute, La Jolla, CA, USA) and housed in the Laboratory Animal Care Facility at the Charles River Campus of Boston University on a 12:12 hour light-dark cycle. All animal procedures were approved by IACUC at Boston University (permit number 13–055) and conducted to minimize animal suffering at all times. Losartan was provided in the drinking water *ad libitum* (600mg/L, Cozaar by Merck pharmaceuticals with 25 g/L of sucrose to increase palatability) beginning at week two until collection at week seven [11]. Typically, animal water consumption is in the range of 1.5ml/10g/day [12]. At seven weeks of age, following 5 weeks of treatment, animals were shipped to University of Florida for skeletal muscle imaging in the Advanced Magnetic Resonance and Spectroscopy (AMRIS) facility. All animals were imaged and euthanized with overdose of Isoflurane within 24 hours of arrival. Hind limb muscles were extracted for histological and biochemical analyses and shipped back to Boston University for further analysis.

MR acquisition

Magnetic resonance imaging (MRI) and spectroscopy (MRS) were performed in a 4.7T horizontal bore magnet (Agilent). The animals were anesthetized using an oxygen and isoflurane mixture (3% isoflurane) and maintained under 0.5–1% isoflurane for the duration of the MR procedure. Respiratory rate and body temperature of the mice were monitored for the entire duration of the scan. The lower hindlimbs of the mice were inserted up to the knee into a 2.0 cm internal diameter, custom-built solenoid ^{1}H coil (200 MHz). T_2-weighted MR multiple slice, single-spin echo images were acquired with the following parameters: repetition time (TR): 2,000ms; echo time (TE): 14ms and 40ms; FOV: 10-20mm; slice thickness: 1mm; acquisition matrix: 128 x 256; and two signal averages [13]. Hahn spin echoes were implemented to avoid the contribution of stimulated echoes in the T_2 measurement. T_2 was determined assuming a single exponential decay. Based on our previous work, we find that calculating T_2 from two echoes is sufficient to differentiate between healthy and damaged muscle [13, 14]. Signal to noise ratios (SNR) were 33:1 at TE = 14ms and 12:1 at TE = 40ms. Additionally, ^{1}H spectroscopic relaxometry was determined from a single voxel within the posterior muscle compartment using Stimulated Echo Acquisition Mode (STEAM) with the following parameters: typical voxel size of 1.5x3.0x1.5; repetition time (TR): 9,000ms; echo time (TE): 5, 6, 7, 8, 9, 10, 15, 20, 25, 30, 35, 40, 45, 50, 55, 60, 65, 70, 80, 90, 100, 110, 120, 130, 140, 150, 160, 170, and 200ms; mixing time (T_M): 20ms; and number of phase cycled averages = 4. Furthermore, three-dimensional gradient echo (3D-GRE, T_1 weighted) images were acquired at 4.7T with the following parameters: field of view: 15x15x15 mm^3; matrix size: 256x192x96; TR/TE = 50/7ms; number of averages: 2; flip angle: 40°.

MR analysis

Images were converted to Digital Imaging and Communication in Medicine (DICOM) format using a custom-made IDL code for Varian data (IDL, ITT Visual Information Systems, Boulder, CO). Anterior and posterior compartments were outlined on axial images of the whole limb to determine the volume of individual compartments. Furthermore, muscle T_2 values of anterior and posterior compartment were computed and analyzed using T_2 maps, created from two echo times (TEs 14ms and 40ms) using OsiriX (Version 3.9.4, Geneva, Switzerland), an open-source software. Muscle T_2 was calculated from 6–8 middle MR images. Imaging-based T_2 was

calculated using the following equation: T_2 = (26ms)/ ln (SI_{14}/SI_{40}), where SI_{14} and SI_{40} are the image pixel intensities at TE of 14ms and 40ms, respectively. Additionally, imaging T_2 values of the muscle were calculated from T_2 maps by excluding the pixels that had T_2 values greater than 2 standard deviations above the mean muscle T_2 value found in control mice (>27ms) (defined as hyperintense throughout the manuscript). Finally, the muscle water-only (^1H_2O) T_2 data was analyzed using a custom-written software (IDL; Exelis VIS, Herndon, VA). Specifically, ^1H_2O relaxation time was derived from the decay in H_2O signal at non-linear spaced echo times (TEs: 5, 6, 7, 8, 9, 10, 15, 20, 25, 30, 35, 40, 45, 50, 55, 60, 65, 70, 80, 90, 100, 110, 120, 130, 140, 150, 160, 170, and 200ms) using complex principal component analysis [7, 15]. ^1H_2O T_2 was determined by a non-linear curve fitting the decay in water signal as a function of TE using a mono-exponential model [16, 17] as well as using non-negative least squares (T_2-NNLS) [18].

Hematoxylin and Eosin (H&E) Staining

Tibialis anterior and Gastrocnemius-Soleus muscle were embedded in TissueTek OCT compound (Sakura Finetek, Torrance, CA, USA) and frozen using isopentane chilled in liquid nitrogen. 7μM frozen sections of TA and GS were obtained from the midbelly region of the TA muscle using a Leica CM 1850 cryostat. Sections were air-dried at room temperature for 5 minutes and fixed in chilled acetone for 5 minutes. They were then hydrated through decreasing grades of alcohol and stained with hematoxylin (Fisher Scientific, Fair Lawn, NJ, USA) for 1 minute, followed by development in 1% ammonium hydroxide for 1 minute. Sections were subsequently stained with Ruben's Eosin-Phloxine working Solution (Biocare Medical LLC) for 2 minutes. After dehydration through increasing grades of alcohol and xylene, sections were mounted using Cytoseal 280 (Richard Allen Scientific, Kalamazoo, MI, USA). Slides were imaged with a Nikon DSFi1 camera head attached to a Nikon ECLIPSE 50i light microscope system and analyzed using NIS-Elements Basic Research 3.0 software.

Picrosirius Staining

Picrosirius Red (American MasterTech Scientific, Inc., Lodi, CA, USA) staining was performed on TA and GS according to the manufacturer's instructions. Sections were fixed with chilled acetone for 5 minutes and then rehydrated through decreasing grades of alcohol. Rehydrated sections were stained with Picrosirius red solution for 15 minutes, rinsed twice in 0.5% acetic acid, and then dehydrated in increasing grades of alcohol and subsequently cleared in xylene. The sections were mounted using Cytoseal 280.

Immunohistochemistry

Frozen tissue sections were fixed in acetone for 15 minutes then left to air dry for 15 minutes. Protocol for Mouse on Mouse (M.O.M.) serial immunostaining for frozen sections provided by Vector Labs (Burlingame, CA) was followed using anti-CD11b (Mac-1) (BD Biosciences, Franklin Lakes, NJ). Sections were then stained with DAPI and mounted with 2:1 Glycerol:PBS mixture and imaged with a Nikon DSFi1 camera head attached to a Nikon ECLIPSE 50i light microscope system. These images were analyzed using NIS-Elements Basic Research 3.0 software. IHC quantification was completed by averaging Mac-1 positive cells on three separate 40x field views per sample.

Gene Expression

RNA from 25mg liquid nitrogen of snap-frozen pooled hind limb muscles (TA, GS) from individual animals was extracted with TRIzol reagent (Invitrogen, Carlsbad, CA) according to the

manufacturer's instructions. Reverse transcription was completed with the High Capacity cDNA Reverse Transcription Kit (Applied Biosystems, Foster City, CA, USA) using 1μg of RNA. Gene expression analysis was completed using TaqMan assays (Applied Biosystems, Foster City, CA, USA) on an ABI 7300 Real Time PCR system. 18s ribosomal subunit RNA served as the endogenous control and gene expression was calculated using the ΔΔCt method.

Statistical Analysis

Statistical analyses were performed using GraphPad Prism 6 Software (GraphPad Software, La Jolla, CA, USA) and included one way analysis of variance (ANOVA) followed by Tukey's multiple comparisons test. All data are presented as mean ± standard deviation. Statistical significance was set at $p<0.05$. Number of mice used in the study are as follows: WT n = 6, DyW n = 8, and DyW Losartan-treated n = 4)

Results

MRI is able to detect differences (or lack thereof) in muscle volume of treated and untreated DyW mice

It has been previously shown that Losartan does not have a significant effect on bodyweight in DyW mice [19]. Indeed, at 7 weeks of age, we did not observe any difference in body weight between untreated DyW (10.11±3.39g) and Losartan-treated DyW mice (10.35 ±1.85g) with both groups being significantly smaller than age-matched WT littermates (18.05 ± 2.91g) ($p<0.05$, one-way ANOVA) (Fig 1A). The same trend was seen for muscle size; MR images qualitatively show that DyW mice have much smaller hind limb muscles as well as many areas of hyperintense pixels on T_2-weighted images not evident in WT muscle. While Losartan-treated hind limbs do not exhibit increases in overall muscle size, they do show attenuation of MR hyperintense areas compared to untreated DyW mice (Fig 1E). To quantify muscle size, 3D T_1 weighted MRI was utilized. Muscle volumes of both anterior and posterior hind limb compartments of DyW mice were significantly smaller than WT counterparts ($p<0.0001$, one-way ANOVA) (Fig 1D). Losartan did not induce increased muscle volume in either compartment compared to untreated DyW mice, which is also reflected in muscle weights and cross-sectional areas (Fig 1B and 1C). These results firstly confirm, using MRI, what previous studies have shown that Losartan does not induce change in overall size/muscle weight [20]. Secondly, 3D MRI can readily detect differences (or lack thereof) in muscle size in mice as small as DyW.

MR quantifications are sensitive to inflammatory and fibrotic attenuation in DyW mice and coincide with histological/biochemical analyses

It has been shown that DyW mice have a severe inflammatory pathology due to large numbers of infiltrating cells [21–23]. As previously stated, it can be seen in MR images that DyW mice exhibit many areas of hyperintensity (indicative of areas of inflammation and edema) [24] that are not evident in WT muscle, and that Losartan-treated hind limbs do not show the same extent of T_2 hyperintensity (Fig 1E). Interestingly, Losartan treatment has been shown to reduce inflammatory cell infiltration [11, 19]. Quantification of DyW posterior compartment muscle T_2 showed a significantly elevated T_2 compared to WT (Fig 2A) (27.10 ± 1.38ms vs. 24.83 ± 0.66ms; $p<0.01$, one-way ANOVA). Following treatment with Losartan, we observed a significant decrease in muscle T_2 values between DyW and DyW-Losartan-treated mice (27.10 ± 1.38ms vs. 23.92 ± 0.80ms; $p<0.001$, one-way ANOVA). This was further confirmed using highly TE sampled, localized ^1H_2O MRS quantification, which demonstrated a similar

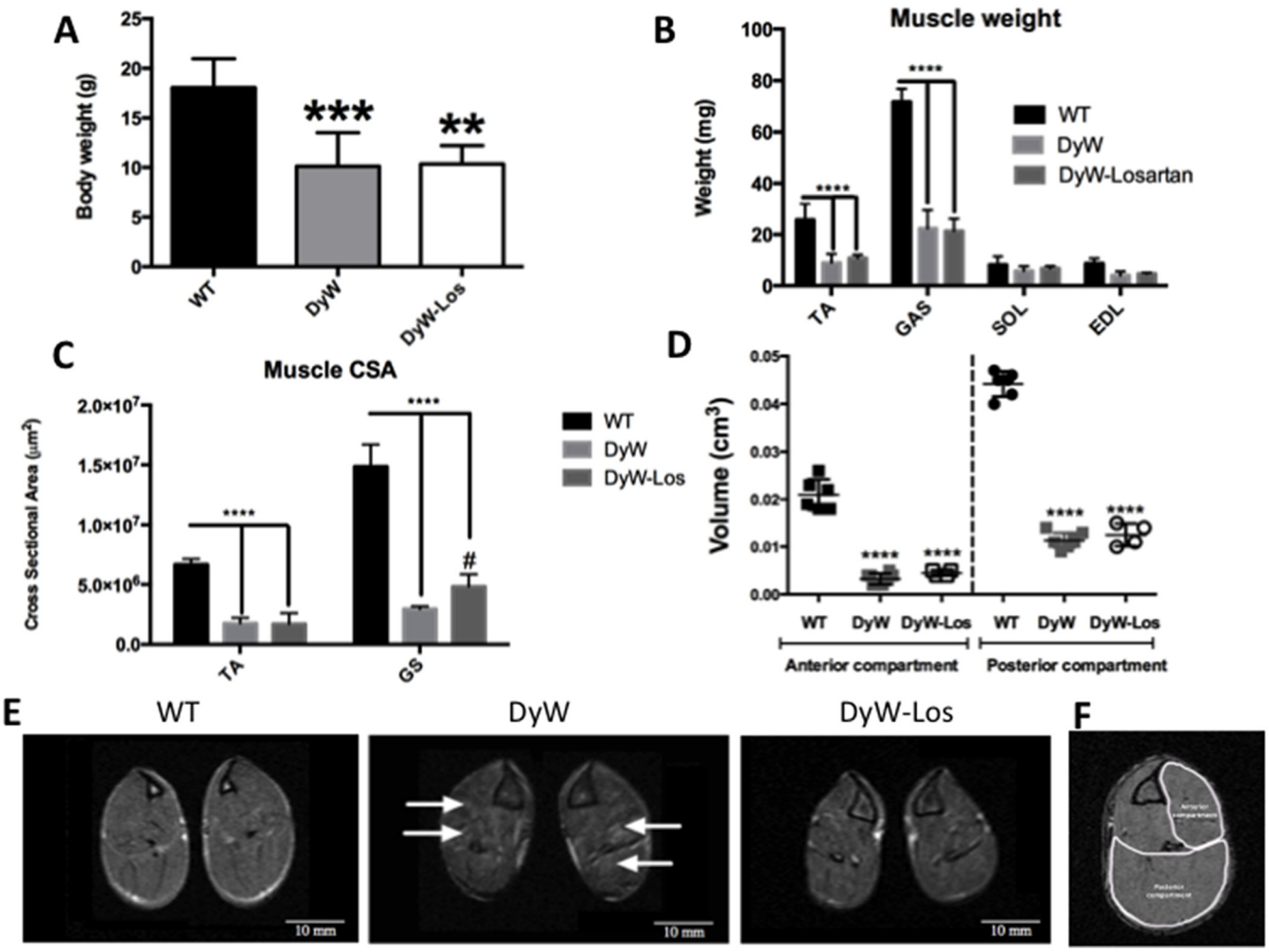

Fig 1. MRI is able to detect differences (or lack thereof) in DyW muscle volume. A) At 7 weeks of age, DyW mice weigh significantly less than age-matched WT littermates ($p<0.001$, one-way ANOVA). Losartan treatment had no effect on DyW total bodyweight. B-C) Hind limb muscles (Tibialis Anterior, Gastrocnemius, Soleus, Extensor Digotorum Longus) from untreated DyW are significantly smaller than WT muscles in terms of weight ($p<0.0001$, one-way ANOVA) and cross-sectional area (CSA) ($p<0.0001$, one-way ANOVA). Losartan treatment had no effect on TA muscle weight/CSA but did result in a significant increase in GS CSA ($p<0.05$, one-way ANOVA). D) 3D T_1-weighted MR analysis shows that both anterior and posterior compartments of DyW hind limb muscle are significantly smaller in terms of volume than WT mice ($p<0.0001$, one-way ANOVA). Similar to total bodyweight, Losartan had no effect on either anterior or posterior compartment muscle volume. E) MR images of WT, DyW, and Losartan-treated DyW mice show that DyW muscle is much smaller than WT and exhibit multiple areas of hyperintensity (indicated by arrows) on T2 weighted MR images. F) Outline of anterior and posterior compartments. (* is used to denote significance between WT and DyW; # is used to denote significance between DyW and DyW Losartan-treated; * = $p<0.05$, ** = $p<0.01$, *** = $p<0.001$, **** = $p<0.0001$, this also applies to the other symbols). WT n = 6, DyW n = 8, DyW Losartan-treated n = 4.

doi:10.1371/journal.pone.0138254.g001

trend thereby validating the use of MR as a non-invasive tool to detect differences in inflammatory pathology in DyW mice (Fig 2B) using both imaging and spectroscopic methods.

Changes in T_2 values were compared with histological and biochemical analyses of the same tissues. H&E staining shows DyW mice have large areas of inflammation and edema with infiltrating cells in both posterior compartment (GS) (2C), and anterior compartment muscle (TA) (Fig 2D) whereas these areas are absent in WT mice. Muscles of DyW mice also have significantly more Mac-1-positive cells (Fig 3A–3D) (3.915 vs. 19.33, $p<0.0001$, one-way ANOVA). In response to Losartan treatment, the number of Mac-1-positive infiltrating cells are significantly reduced back to WT levels (19.33 (DyW) vs. 8.585 (DyW-Los) vs. 3.915 (WT) $p<0.001$,

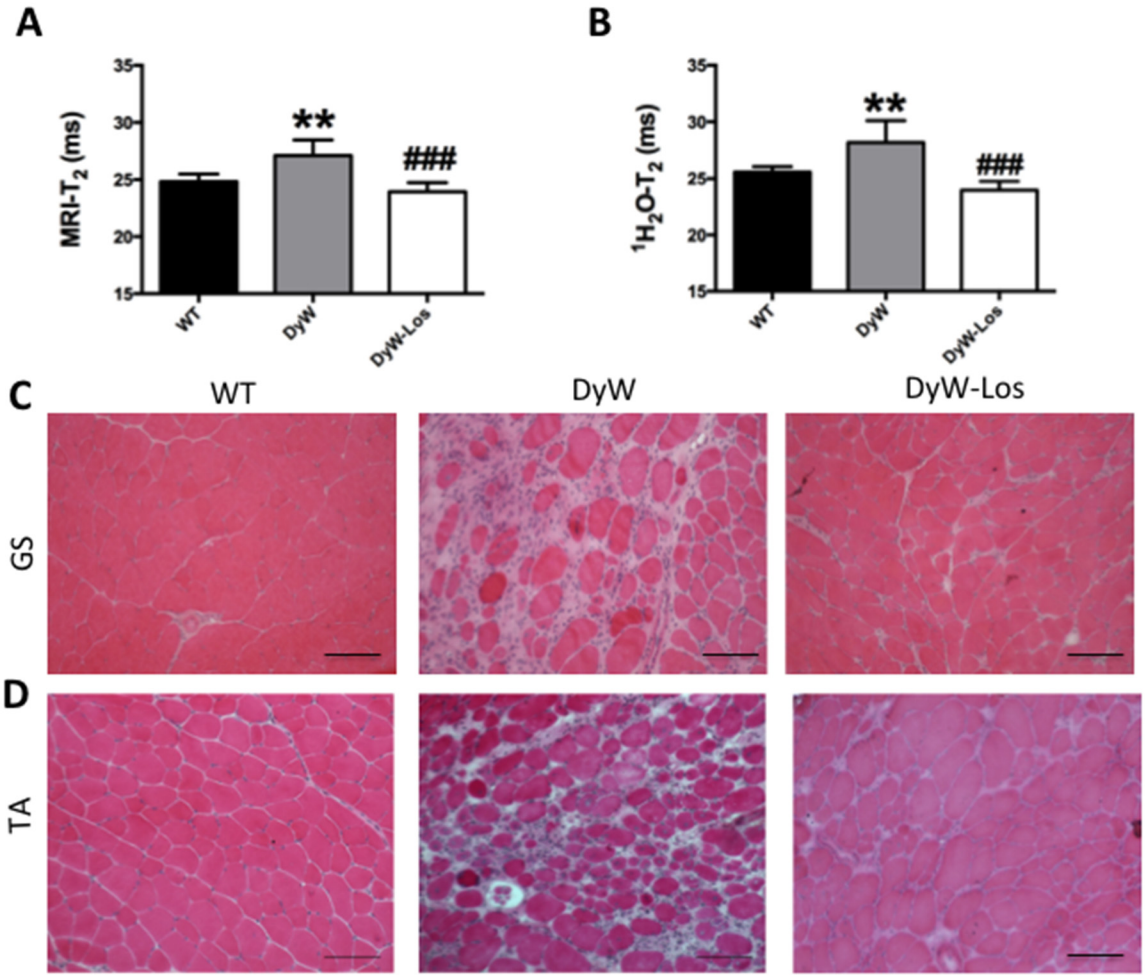

Fig 2. MR analyses are sensitive to and coincide with inflammatory pathology and resolution in DyW mice. A) T_2 weighted MRI of the entire DyW posterior compartment hind limb muscles is significantly elevated compared to age-matched WT littermates ($p<0.01$, one-way ANOVA) indicative of inflammation/edema. Losartan treatment significantly reduced T_2 values to WT levels ($p<0.001$, one-way ANOVA). B) DyW mice also exhibit significantly greater localized ^1H_2O T2 levels compared to WT counterparts ($p<0.01$, one-way ANOVA) which was also significantly lowered in response to Losartan treatment ($p<0.001$, one-way ANOVA). C-D) Histological analyses verified elevated T_2 levels were due to muscle inflammation and edema. H&E staining shows extensive infiltration of inflammatory cells in DyW muscle compared to WT in both GS (C) and TA (D). Note: H&E images taken at 20x magnification. (* is used to denote significance between WT and DyW; # is used to denote significance between DyW and Losartan-treated DyW; * = $p<0.05$, ** = $p<0.01$, *** = $p<0.001$, **** = $p<0.0001$, this also applies to the other symbols). WT n = 6, DyW n = 8, DyW Losartan-treated n = 4.

doi:10.1371/journal.pone.0138254.g002

one-way ANOVA). These analyses corroborate the fact that elevated T_2 values in DyW muscle may in fact be due to increased inflammation, which are attenuated in response to Losartan.

Additionally, it has been established that Losartan is also a potent anti-fibrotic agent [19, 25, 26]. A pixel-by-pixel analysis of DyW T_2 maps indicated that muscle T_2 values were significantly lower when only considering muscle pixels without areas of T_2 elevation (27.10 ± 1.38ms vs. 21.20 ± 0.68ms; $p<0.0001$, one-way ANOVA), suggestive of fibrosis (Fig 4A) [27]. In the case of Losartan-treated mice, pixel-by-pixel analysis of the muscle pixels without T2 elevation, revealed that muscle T_2 values were returned to WT levels (21.20 ± 0.68ms vs. 23.91 ± 0.84ms; $p<0.001$, one-way ANOVA) (Fig 4A) thus demonstrating that MR indices can also detect differences in fibrosis in DyW mice in addition to inflammation. The reduction of fibrosis suggested by normalized muscle-specific T_2 values in response to Losartan was confirmed with Picrosirius red staining which shows markedly increased fibrotic tissue in DyW

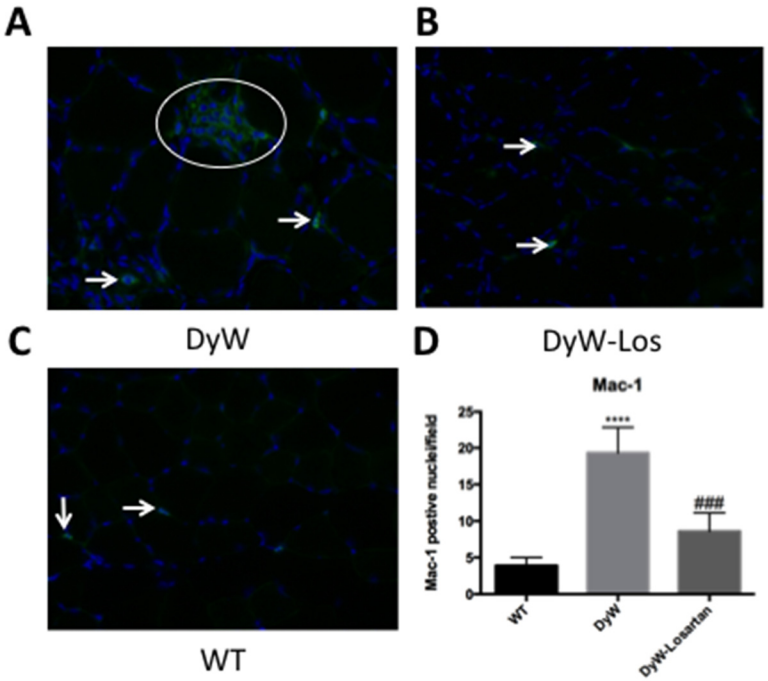

Fig 3. Mac-1 staining confirms inflammatory resolution suggested by MRI quantifications in Losartan-treated DyW mice. A-D) Mac-1 (anti-CD11b) staining shows that there is a significant increase in Mac-1 positive cells in DyW muscle compared to WT ($p<0.0001$, one-way ANOVA). Losartan treatment significantly reduced the amount of Mac-1 positive cell infiltration in DyW muscle ($p<0.001$, one-way ANOVA). (* is used to denote significance between WT and DyW; # is used to denote significance between DyW and Losartan-treated DyW; * = $p<0.05$, ** = $p<0.01$, *** = $p<0.001$, **** = $p<0.0001$, this also applies to the other symbols). WT n = 6, DyW n = 8, DyW Losartan-treated n = 4.

doi:10.1371/journal.pone.0138254.g003

mice compared to WT (Fig 4C). These results were further supported by COL1a overexpression in DyW mice ($p<0.0001$, one-way ANOVA) that returned to WT levels in response to Losartan ($p<0.001$, one-way ANOVA) (Fig 4B).

Discussion

In this study, MRI was utilized to monitor changes in muscle pathology and size in DyW mice in response to treatment with the Angiotensin II type I receptor blocker Losartan. Based on T_1-weighted MR analyses, Losartan treatment did not result in muscle volume changes in DyW mice. On the other hand, Losartan treatment did normalize muscle T_2 values to WT levels. These findings were further confirmed by histological and biochemical analysis showing that MR measurements are sensitive to and reflect therapeutic improvements in DyW muscles.

Losartan has been shown to exhibit both anti-inflammatory and anti-fibrotic effects. Muscle T_2 has been shown to be elevated during inflammation [24] and decreased with fibrosis [27]. In this study we found MR evidence of both decreased inflammation and fibrosis in Losartan-treated DyW muscle. Compared to untreated DyW mice, Losartan-treated mice had decreased total muscle compartment T_2 values suggesting a decrease in inflammation following Losartan treatment. This was confirmed by a reduction in Mac-1 positive cells in treated DyW muscles. Moreover, it has been shown that fibrotic lesions—more specifically lesions with large amounts of collagen buildup—have a lower T_2 signal intensity [28–30]. Cardiac MRI studies in DMD subjects have reported an age related decrease in myocardial T_2 compared to controls [31, 32] and an increase in myocardial T_2 heterogeneity [33]. Similar results have been observed in

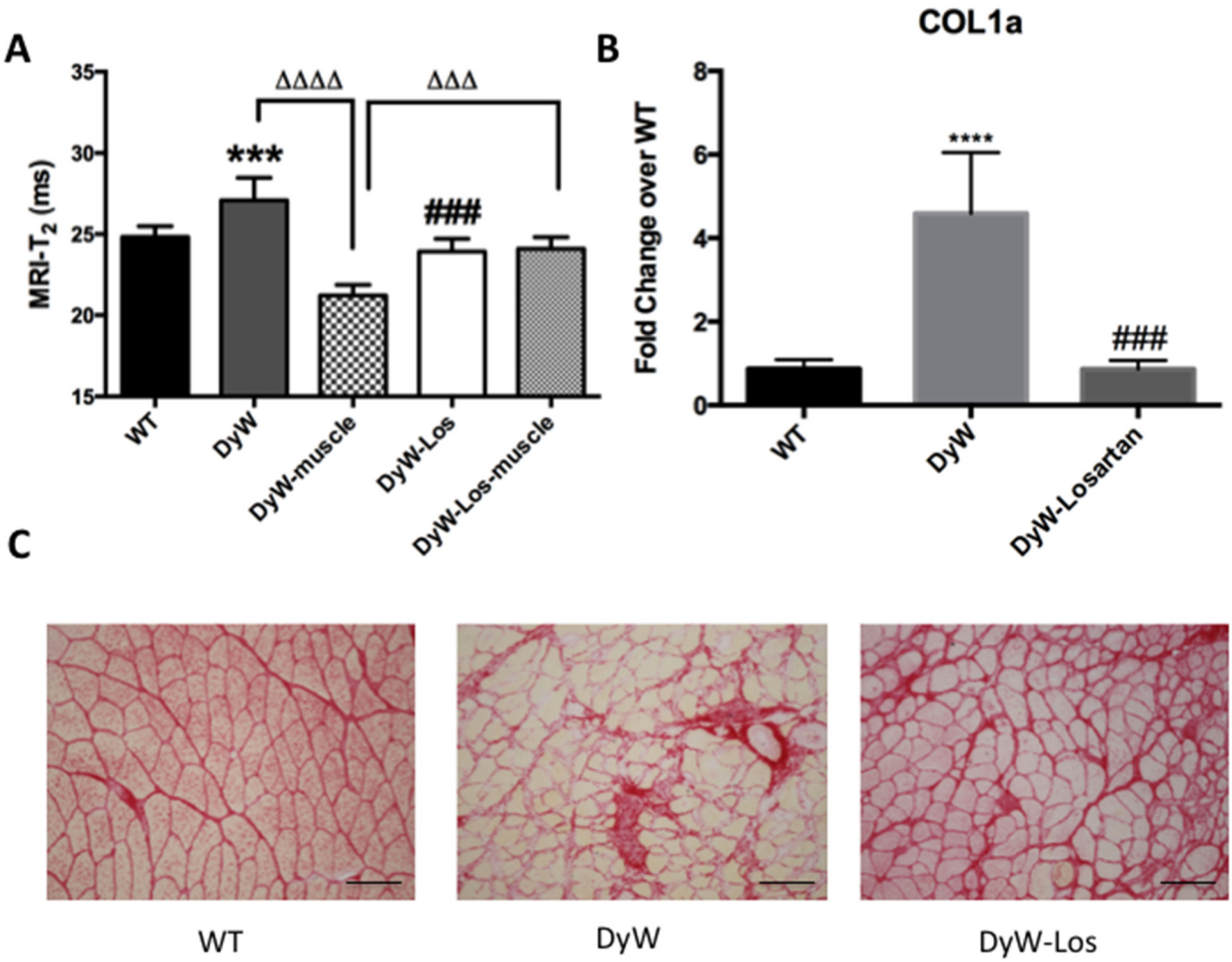

Fig 4. MR analyses are sensitive to and correlate with fibrotic pathology and resolution in DyW mice. A) When areas of hyperintensity are removed from whole posterior compartment T_2 levels, DyW mice show significantly reduced T_2 levels compared to WT ($p<0.0001$, one-way ANOVA). Mice treated with Losartan do not exhibit this reduction of T_2 values following removal of hyperintense areas. B) Because reduced T_2 levels are indicative of fibrosis, specifically collagen buildup, qRT-PCR was used to assess COL1a gene expression. DyW mice exhibit significantly greater gene expression of COL1a compared to age-matched WT littermates ($p<0.0001$, one-way ANOVA), which was rescued back to WT levels in response to treatment with Losartan ($p<0.001$, one-way ANOVA). C) Picrosirius red staining of GS confirms extensive fibrosis in DyW mice that is rescued by Losartan treatment. Picrosirius red images taken at 20x. (* is used to denote significance between WT and DyW; # is used to denote significance between DyW and DyW Losartan-treated; Δ is used to denote significance between DyW and DyW-muscle (with removal of hyperintensive areas); & is used to denote significance between DyW-muscle and DyW Losartan-treated muscle; * = $p<0.05$, ** = $p<0.01$, *** = $p<0.001$, **** = $p<0.0001$, this also applies to the other symbols). WT n = 6, DyW n = 8, DyW Losartan-treated n = 4.

doi:10.1371/journal.pone.0138254.g004

animal models with diabetic induced cardiac fibrosis [27, 34]. The trend of decreased T_2 levels due to fibrosis was also seen in the current MRI examination of DyW hind limb skeletal muscle. When pixels with elevated T_2 values were excluded from the T_2 analyses, muscle T_2 values in DyW mice demonstrated a significant decrease, suggestive of fibrotic tissue buildup [35]. Interestingly, when DyW mice were treated with Losartan, muscle T_2 values were returned to WT levels. These observations were validated by both histological and biochemical analyses that demonstrated Losartan-treated mice exhibit significantly less COL1a gene expression as well as decreased interstitial fibrosis as seen with Picrosirius red staining.

The MR results presented in this study firstly corroborate previous publications demonstrating the positive effects of Losartan in dystrophic models [20, 36]. We previously found and have replicated in this study that Losartan does not have a measurable effect on total body or

muscle weight but does ameliorate fibrotic and inflammatory pathologies. This suggests that an anabolic therapy should be utilized in conjunction with Losartan treatment to achieve comprehensive pathological attenuation. We have previously shown that Insulin-like Growth Factor-1 (IGF-1) overexpression can result in increased muscle mass [35]. In yet another study it has been shown that Adeno-Associated Virus-driven over-expression of IGF-1 can be monitored using MRI muscle measures [37].

The current study provides proof of concept that MRI can quantify muscle mass and composition in small animal models and is able to detect changes in muscle pathology that concur with histological and biochemical analyses, and thus should be considered as a viable and effective non-invasive method of assessing therapeutic efficacy in preclinical studies.

Acknowledgments

We would like to thank Younghwa Rhee and Alex Miller for valuable comments on manuscript revision. We would also like to acknowledge the assistance of Abhinandan Batra, Brittany Lee-McMullen, and Stephen Chrzanowski.

All primary data will be freely available upon request.

Author Contributions

Conceived and designed the experiments: RV AA AK GW MG. Performed the experiments: RV AA AK GW MG. Analyzed the data: RV AA AK GW MG. Contributed reagents/materials/analysis tools: RV AA AK GW MG. Wrote the paper: RV AA AK GW MG.

References

1. Patton B, Miner J, Chiu A, Sanes J. Distribution and function of laminins in the neuromuscular system of developing, adult, and mutant mice. The Journal of cell biology. 1997; 139:1507–21. doi: 10.1083/jcb.139.6.1507 PMID: 9396756
2. Connolly AM, Keeling RM, Mehta S, Pestronk A, Sanes JR. Three mouse models of muscular dystrophy: the natural history of strength and fatigue in dystrophin-, dystrophin/utrophin-, and laminin alpha2-deficient mice. Neuromuscular disorders: NMD. 2001; 11(8):703–12. PMID: 11595512.
3. Tome FM, Evangelista T, Leclerc A, Sunada Y, Manole E, Estournet B, et al. Congenital muscular dystrophy with merosin deficiency. Comptes rendus de l'Academie des sciences Serie III, Sciences de la vie. 1994; 317(4):351–7. PMID: 8000914.
4. Rooney JE, Gurpur PB, Burkin DJ. Laminin-111 protein therapy prevents muscle disease in the mdx mouse model for Duchenne muscular dystrophy. Proceedings of the National Academy of Sciences of the United States of America. 2009; 106(19):7991–6. doi: 10.1073/pnas.0811599106 PMID: 19416897; PubMed Central PMCID: PMC2683113.
5. Philpot J, Bagnall A, King C, Dubowitz V, Muntoni F. Feeding problems in merosin deficient congenital muscular dystrophy. Arch Dis Child. 1999; 80(6):542–7. PMID: 10332004; PubMed Central PMCID: PMCPMC1717951.
6. Pratt SJ, Xu S, Mullins RJ, Lovering RM. Temporal changes in magnetic resonance imaging in the mdx mouse. BMC research notes. 2013; 6(1):262. doi: 10.1186/1756-0500-6-262 PMID: 23837666; PubMed Central PMCID: PMC3716616.
7. Forbes SC, Willcocks RJ, Triplett WT, Rooney WD, Lott DJ, Wang DJ, et al. Magnetic resonance imaging and spectroscopy assessment of lower extremity skeletal muscles in boys with Duchenne muscular dystrophy: a multicenter cross sectional study. PloS one. 2014; 9(9):e106435. doi: 10.1371/journal.pone.0106435 PMID: 25203313; PubMed Central PMCID: PMC4159278.
8. Girgenrath M, Dominov JA, Kostek CA, Miller JB. Inhibition of apoptosis improves outcome in a model of congenital muscular dystrophy. The Journal of clinical investigation. 2004; 114(11):1635–9. doi: 10.1172/JCI22928 PMID: 15578095; PubMed Central PMCID: PMC529286.
9. Kuang W, Xu H, Vachon PH, Liu L, Loechel F, Wewer UM, et al. Merosin-deficient congenital muscular dystrophy. Partial genetic correction in two mouse models. The Journal of clinical investigation. 1998; 102(4):844–52. doi: 10.1172/JCI3705 PMID: 9710454; PubMed Central PMCID: PMC508948.

10. Miyagoe Y, Hanaoka K, Nonaka I, Hayasaka M, Nabeshima Y, Arahata K, et al. Laminin alpha2 chain-null mutant mice by targeted disruption of the Lama2 gene: a new model of merosin (laminin 2)-deficient congenital muscular dystrophy. FEBS letters. 1997; 415(1):33–9. PMID: 9326364.

11. Cohn RD, van Erp C, Habashi JP, Soleimani AA, Klein EC, Lisi MT, et al. Angiotensin II type 1 receptor blockade attenuates TGF-beta-induced failure of muscle regeneration in multiple myopathic states. Nat Med. 2007; 13(2):204–10. Epub 2007/01/24. nm1536 [pii] doi: 10.1038/nm1536 PMID: 17237794.

12. Bachmanov AA, Reed DR, Beauchamp GK, Tordoff MG. Food intake, water intake, and drinking spout side preference of 28 mouse strains. Behavior genetics. 2002; 32(6):435–43. PMID: 12467341; PubMed Central PMCID: PMC1397713.

13. Vohra RS, Mathur S, Bryant ND, Forbes S, Vandenborne K, Walter GA. Age-related T changes in hindlimb muscles of mdx mice. Muscle Nerve. 2015. doi: 10.1002/mus.24675 PMID: 25846867.

14. Mathur S, Vohra RS, Germain SA, Forbes S, Bryant ND, Vandenborne K, et al. Changes in muscle T2 and tissue damage after downhill running in mdx mice. Muscle Nerve. 2011; 43(6):878–86. doi: 10.1002/mus.21986 PMID: 21488051; PubMed Central PMCID: PMC3101319.

15. Elliott MA, Walter GA, Swift A, Vandenborne K, Schotland JC, Leigh JS. Spectral quantitation by principal component analysis using complex singular value decomposition. Magnetic resonance in medicine: official journal of the Society of Magnetic Resonance in Medicine / Society of Magnetic Resonance in Medicine. 1999; 41(3):450–5. PMID: 10204865.

16. Fisher MJ, Meyer RA, Adams GR, Foley JM, Potchen EJ. Direct relationship between proton T2 and exercise intensity in skeletal muscle MR images. Investigative radiology. 1990; 25(5):480–5. PMID: 2345077.

17. Walter G, Cordier L, Bloy D, Sweeney HL. Noninvasive monitoring of gene correction in dystrophic muscle. Magnetic resonance in medicine: official journal of the Society of Magnetic Resonance in Medicine / Society of Magnetic Resonance in Medicine. 2005; 54(6):1369–76. doi: 10.1002/mrm.20721 PMID: 16261578.

18. Saab G, Thompson RT, Marsh GD. Multicomponent T2 relaxation of in vivo skeletal muscle. Magnetic resonance in medicine: official journal of the Society of Magnetic Resonance in Medicine / Society of Magnetic Resonance in Medicine. 1999; 42(1):150–7. PMID: 10398961.

19. Elbaz M, Yanay N, Aga-Mizrachi S, Brunschwig Z, Kassis I, Ettinger K, et al. Losartan, a therapeutic candidate in congenital muscular dystrophy: Studies in the dy(2J) /dy(2J) Mouse. Ann Neurol. 2012; 71:699–708. doi: 10.1002/ana.22694 PMID: 22522482

20. Elbaz M, Yanay N, Aga-Mizrachi S, Brunschwig Z, Kassis I, Ettinger K, et al. Losartan, a therapeutic candidate in congenital muscular dystrophy: studies in the dy(2J) /dy(2J) mouse. Ann Neurol. 2012; 71 (5):699–708. Epub 2012/04/24. doi: 10.1002/ana.22694 PMID: 22522482.

21. Hayashi YK, Tezak Z, Momoi T, Nonaka I, Garcia CA, Hoffman EP, et al. Massive muscle cell degeneration in the early stage of merosin-deficient congenital muscular dystrophy. Neuromuscular disorders: NMD. 2001; 11(4):350–9. PMID: 11369186.

22. Mourkioti F, Rosenthal N. NF-kappaB signaling in skeletal muscle: prospects for intervention in muscle diseases. Journal of molecular medicine. 2008; 86(7):747–59. doi: 10.1007/s00109-008-0308-4 PMID: 18246321; PubMed Central PMCID: PMC2480606.

23. Mehuron T, Kumar A, Duarte L, Yamauchi J, Accorsi A, Girgenrath M. Dysregulation of matricellular proteins is an early signature of pathology in laminin-deficient muscular dystrophy. Skelet Muscle. 2014; 4:14. doi: 10.1186/2044-5040-4-14 PMID: 25075272; PubMed Central PMCID: PMCPMC4114446.

24. Bryant ND, Li K, Does MD, Barnes S, Gochberg DF, Yankeelov TE, et al. Multi-parametric MRI characterization of inflammation in murine skeletal muscle. NMR in biomedicine. 2014; 27(6):716–25. doi: 10.1002/nbm.3113 PMID: 24777935; PubMed Central PMCID: PMC4134016.

25. Spurney CF, Sali A, Guerron AD, Iantorno M, Yu Q, Gordish-Dressman H, et al. Losartan decreases cardiac muscle fibrosis and improves cardiac function in dystrophin-deficient mdx mice. Journal of cardiovascular pharmacology and therapeutics. 2011; 16(1):87–95. doi: 10.1177/1074248410381757 PMID: 21304057; PubMed Central PMCID: PMC4147941.

26. Bish LT, Yarchoan M, Sleeper MM, Gazzara JA, Morine KJ, Acosta P, et al. Chronic losartan administration reduces mortality and preserves cardiac but not skeletal muscle function in dystrophic mice. PloS one. 2011; 6(6):e20856. doi: 10.1371/journal.pone.0020856 PMID: 21731628; PubMed Central PMCID: PMC3120761.

27. Bun SS, Kober F, Jacquier A, Espinosa L, Kalifa J, Bonzi MF, et al. Value of in vivo T2 measurement for myocardial fibrosis assessment in diabetic mice at 11.75 T. Invest Radiol. 2012; 47(5):319–23. doi: 10.1097/RLI.0b013e318243e062 PMID: 22488510.

28. Gupta RK, Tomar V, Awasthi R, Yadav A, Husain N, Bharadwaj V, et al. T2*-weighted MR angiography substantially increases the detection of hemorrhage in the wall of brain abscess: implications in clinical

interpretation. Neuroradiology. 2012; 54(6):565–72. doi: 10.1007/s00234-011-0952-1 PMID: 21915689.

29. van Nierop BJ, Bax NA, Nelissen JL, Arslan F, Motaal AG, de Graaf L, et al. Assessment of Myocardial Fibrosis in Mice Using a T2*-Weighted 3D Radial Magnetic Resonance Imaging Sequence. PloS one. 2015; 10(6):e0129899. doi: 10.1371/journal.pone.0129899 PMID: 26115443; PubMed Central PMCID: PMC4482648.

30. Wang J, Xiang B, Lin HY, Liu H, Freed D, Arora RC, et al. Pathological mechanism for delayed hyperenhancement of chronic scarred myocardium in contrast agent enhanced magnetic resonance imaging. PloS one. 2014; 9(5):e96463. doi: 10.1371/journal.pone.0096463 PMID: 24802515; PubMed Central PMCID: PMC4011786.

31. Mavrogeni S, Papavasiliou A, Douskou M, Kolovou G, Papadopoulou E, Cokkinos DV. Effect of deflazacort on cardiac and sternocleidomastoid muscles in Duchenne muscular dystrophy: a magnetic resonance imaging study. Eur J Paediatr Neurol. 2009; 13(1):34–40. doi: 10.1016/j.ejpn.2008.02.006 PMID: 18406648.

32. Mavrogeni S, Tzelepis GE, Athanasopoulos G, Maounis T, Douskou M, Papavasiliou A, et al. Cardiac and sternocleidomastoid muscle involvement in Duchenne muscular dystrophy: an MRI study. Chest. 2005; 127(1):143–8. doi: 10.1378/chest.127.1.143 PMID: 15653975.

33. Wansapura JP, Hor KN, Mazur W, Fleck R, Hagenbuch S, Benson DW, et al. Left ventricular T2 distribution in Duchenne muscular dystrophy. J Cardiovasc Magn Reson. 2010; 12:14. doi: 10.1186/1532-429X-12-14 PMID: 20298602; PubMed Central PMCID: PMC2846924.

34. Loganathan R, Bilgen M, Al-Hafez B, Smirnova IV. Characterization of alterations in diabetic myocardial tissue using high resolution MRI. Int J Cardiovasc Imaging. 2006; 22(1):81–90. doi: 10.1007/s10554-005-5386-6 PMID: 16362172.

35. Kumar A, Yamauchi J, Girgenrath T, Girgenrath M. Muscle-specific expression of insulin-like growth factor 1 improves outcome in Lama2Dy-w mice, a model for congenital muscular dystrophy type 1A. Hum Mol Genet. 2011; 20(12):2333–43. doi: 10.1093/hmg/ddr126 PMID: 21441569; PubMed Central PMCID: PMC3098729.

36. Meinen S, Lin S, Ruegg MA. Angiotensin II type 1 receptor antagonists alleviate muscle pathology in the mouse model for laminin-alpha2-deficient congenital muscular dystrophy (MDC1A). Skeletal muscle. 2012; 2(1):18. doi: 10.1186/2044-5040-2-18 PMID: 22943509; PubMed Central PMCID: PMC3598380.

37. Ye F, Mathur S, Liu M, Borst SE, Walter GA, Sweeney HL, et al. Overexpression of insulin-like growth factor-1 attenuates skeletal muscle damage and accelerates muscle regeneration and functional recovery after disuse. Experimental physiology. 2013; 98(5):1038–52. doi: 10.1113/expphysiol.2012.070722 PMID: 23291913.